Brain, Behavior, & Immunity - Health 32 (2023) 100675

Contents lists available at ScienceDirect

Brain, Behavior, & Immunity - Health

journal homepage: www.editorialmanager.com/bbih/default.aspx

Meditation-induced bloodborne factors as an adjuvant treatment to COVID-19 disease

Juan P. Zuniga-Hertz [a,b,1], Ramamurthy Chitteti [a,b,1], Joe Dispenza [c], Raphael Cuomo [b], Jacqueline A. Bonds [a,b], Elena L. Kopp [a,b], Sierra Simpson [b], Jonathan Okerblom [b], Svetlana Maurya [d], Brinda K. Rana [e], Atsushi Miyonahara [b], Ingrid R. Niesman [f], Jacqueline Maree [g], Gianna Belza [a,b], Hillari D. Hamilton [c], Carla Stanton [c], David J. Gonzalez [d,h], Michelle A. Poirier [g], Tobias Moeller-Bertram [g], Hemal H. Patel [a,b,*]

[a] Veterans Affairs San Diego Healthcare System, 3350 La Jolla Village Drive, San Diego, CA, 92161, USA
[b] Department of Anesthesiology, University of California, San Diego, La Jolla, CA, 92093, USA
[c] Encephalon, Inc., Rainier, WA, 98576, USA
[d] Department of Pharmacology, University of California, San Diego, La Jolla, CA, 92093, USA
[e] Department of Psychiatry, University of California, San Diego, La Jolla, CA, 92093, USA
[f] San Diego State University, Electron Microscope Facility, 5500 Campanile Dr, San Diego, CA, 92182, USA
[g] VitaMed Research, 44630 Monterey Ave., Palm Desert, CA, 92260, USA
[h] Skaggs School of Pharmacy and Pharmaceutical Sciences, University of California, San Diego, La Jolla, CA, 92093, USA

ARTICLE INFO

Keywords:
Meditation
Immunity
Adoptive blood transfer
serpin
SARS-CoV-2
Pseudovirus
COVID-19 disease

ABSTRACT

The COVID-19 pandemic has resulted in significant morbidity and mortality worldwide. Management of the pandemic has relied mainly on SARS-CoV-2 vaccines, while alternative approaches such as meditation, shown to improve immunity, have been largely unexplored. Here, we probe the relationship between meditation and COVID-19 disease and directly test the impact of meditation on the induction of a blood environment that modulates viral infection. We found a significant inverse correlation between length of meditation practice and SARS-CoV-2 infection as well as accelerated resolution of symptomology of those infected. A meditation "dosing" effect was also observed. In cultured human lung cells, blood from experienced meditators induced factors that prevented entry of pseudotyped viruses for SARS-CoV-2 spike protein of both the wild-type Wuhan-1 virus and the Delta variant. We identified and validated SERPINA5, a serine protease inhibitor, as one possible protein factor in the blood of meditators that is necessary and sufficient for limiting pseudovirus entry into cells. In summary, we conclude that meditation can enhance resiliency to viral infection and may serve as a possible adjuvant therapy in the management of the COVID-19 pandemic.

1. Introduction

Emergence and spread of the SARS-CoV-2 pandemic has resulted in over 500 million cases of COVID-19 worldwide, leading to over 6 million deaths (University). Spikes, surges, waves, and variants have continued to upend the normalcy of life over the past two years, impacting work, school, social interactions, travel, and the economy across the globe. Though vaccines are mainstays in well-resourced countries, there is a significant minority of individuals that will not participate in such interventions due to political, ideological, trust, ethnicity, and socio-economic inequity issues in resourced countries and fear of vaccine safety and lack of availability in low and middle income countries (Glazik et al., 2021; Omer et al., 2021). Several experimental compounds have been proposed for the treatment of COVID-19, including hydroxychloroquine, remdesivir, lopinavir, interferon-β1, ivermectin, convalescent plasma; however, many of these treatments result in more harm than overall benefit (Bishara et al., 2020; Buonfrate et al., 2022; Consortium et al., 2021; Ortigoza et al., 2021). No safe, effective,

* Corresponding author. Department of Anesthesiology, University of California, VA San Diego Healthcare System, #125, 3350 La Jolla Village Dr., San Diego, CA, 92161, USA.
E-mail address: hepatel@ucsd.edu (H.H. Patel).
[1] These authors share equal first authorship.

https://doi.org/10.1016/j.bbih.2023.100675
Received 5 December 2022; Received in revised form 12 July 2023; Accepted 6 August 2023
Available online 7 August 2023

easily-applied approach with significant potential to limit initial infection or symptom severity has emerged.

Alternative and complementary approaches such as meditation can improve the stress response and have a range of health benefits, presumably by creating a new tissue and blood environment that enhances health and resilience. However, the latter aspect has not been directly tested. Using such practices generally produces an abundance of benefit with little to no harm potential. While there are many different schools and forms of meditation, such as mindfulness meditation, yoga, and breathing exercises, they all involve mental training with a goal of transcendence of ordinary consciousness (Ospina et al., 2007). Guided meditation is particularly beneficial because the very nature of instruction tends to relate to some specific purpose, such as healing or self-improvement (Ospina et al., 2007). Meditative practices are associated with improvements in mental health conditions such as anxiety and depression and physical symptoms like pain (Bohlmeijer et al., 2010; Shapiro, 2009) and can have positive effects on specific markers of inflammation, cell-mediated immunity, antibody responses, and biological aging (Black et al., 2019). Recent studies carried out in both healthy and clinical populations have begun to shed light on the molecular changes associated with meditation and other mind-body practices (Gomutbutra et al., 2020; Buric et al., 2017). Collectively, these studies have revealed that mindfulness-based practices result in down-regulation of NF-kB, a key regulator of inflammation (Buric et al., 2017), and upregulation of BDNF, a neuronal growth factor implicated in neuronal plasticity (Gomutbutra et al., 2020), and in IRF-1, a gene important in viral defense mechanisms (Feng et al., 2021).

Recently, hypotheses have been proposed to suggest the potential for meditation to modulate SARS-CoV-2 and COVID-19, elegantly reviewed by Mills, Chopra, and colleagues (Bushell et al., 2020). To this end, Chandran et al. have explored the effect of a vegan diet and an intensive 8-day meditation workshop on gene expression (Chandran et al., 2021). Data from this genomic study followed by multilevel bioinformatics analysis demonstrated that this meditative practice leads to an up-regulation of 220 genes associated with immune response and that this meditation-specific network is significantly down-regulated in COVID-19 patients. These data support the hypothesis that meditation can serve as an effective complementary adjuvant therapy for COVID-19 disease.

Here, in an effort to better characterize the impact of meditation on COVID-19, we administered a survey to members of a meditation community who had previously attended a 7-day advanced meditation workshop. To systematically identify possible factors that may be induced by meditative practices employed by this community, we collected blood plasma from attendees of three comparable meditation workshops. Using cultured mammalian lung cells, we examined the effect of this plasma on the infectivity of SARS-CoV-2 pseudovirus, including several variants of concern (VOC). Finally, we carried out proteomics analysis on the plasma to identify potential factors induced by meditation that may be specifically involved in protection against viral infectivity.

2. Materials and methods

2.1. Survey data collection

After Institutional Review Board (IRB) review by the Western IRB (now WCG-IRB), an internet survey platform was utilized to administer a COVID-19-related survey online. Data were collected in accordance with ethical guidelines pertaining to the use of human subjects. This survey instrument was designed to assess mediation-related behaviors and COVID-19 outcomes in a selective meditation community, as well as potential confounders and mediators of these exposures and outcomes. In addition, participants were asked about their general health status, history of positive or negative COVID-19 diagnosis, symptoms experienced (if any), and current vaccination status. Meditation-related behavioral covariates included length of experience with meditation practice and frequency of meditation practice. Variables generated for COVID-19 outcomes included self-assessed COVID-19 infection, COVID-19 symptoms, duration of COVID-19 infection, COVID-19 vaccination status, and experience of long-term symptoms. Data were also collected on respondent demographics (race/ethnicity, sex, age), self-attribution as a current or former smoker, and medical comorbidities (cancer, stroke, diabetes, heart disease, vascular disease, lung disease, kidney disease, liver disease, autoimmune disease, neurological disorder, and obesity). Additionally, data were available for the respondent location. Consent to participate in meditation-related research was obtained through the survey instrument itself.

Available subject sampling was used to disseminate surveys to a cohort of 22,459 individuals that had previously attended a 7-day meditation-related workshop. Therefore, the sampling frame for surveying was a population of individuals who had attended this 7-day meditation workshop. Stratified sampling was not conducted, as the purpose of the survey was to understand the relationship between meditation-related behaviors and outcomes related to COVID-19. The purpose of surveying was not to understand variations in these behaviors and outcomes across subgroups of meditators, though differences in the relationship between these factors was assessed through stratification during the data analysis phase. Quota groups and exclusion criteria were not programmed into the survey instrument.

2.2. Survey data analysis

Subject-Level Analysis: Bivariate regressions were conducted to assess whether COVID-19 outcomes differed significantly for respondents across meditation-related behaviors. In addition, multivariable logistic regression models were computed to predict COVID-19 infection. Backwards selection using the Wald statistic was performed, and Nagelkerke's R^2 and AIC were computed in a stepwise fashion to assess model fit. All analyses were done in SPSS version 27 (IBM: Armonk, New York).

Geospatial Analysis: Geospatial data were used to stratify respondents to determine if attendees of the workshop from different areas exhibited different COVID-19-related outcomes in response to meditation. The purpose of this analysis was not to obtain representative statistics of behaviors or disease outcomes from different geospatial areas, but rather to understand whether subject-level relationships between meditation behaviors and COVID-19 outcomes were retained when workshop participants were grouped into geospatial strata.

Country, first-level subnational unit (e.g., states/provinces), and city of residence were manually entered by respondents. These were manually reviewed by the authors for misspellings, concatenated into one string per respondent, and processed using the Google Maps API to generate latitude and longitude coordinates. These were plotted on a projected coordinate plane and manually reviewed for face validity, after which they were aggregated to polygons in a shapefile of geospatial units. In order to ensure robust statistical analysis, geospatial units were grouped such that they had a minimum of 10 respondents ($n \geq 10$), which is considered a sufficiently high sample size to minimize sampling bias while also allowing for meaningful comparisons between the groups. Aggregation was conducted first at the country-level, and then at the first-level subnational entity for countries with $n > 200$ survey responses (United States), and finally at the county level for first-level subnational entities with $n > 200$ survey responses (California, Florida). Percentages for meditation-related behaviors and COVID-19 outcomes were computed for each geospatial unit. Linear regression was conducted to determine the bivariate relationship between meditation-related behaviors and COVID-19-related outcomes across geospatial strata among participants who attended this meditation workshop. Statistical power was not available for multivariable modeling at the ecological level, though these were conducted at the respondent level. All data used for both subject-level and geospatial analyses were

obtained from the survey; no secondary data relating to COVID-19 rates or meditation behaviors were utilized in this analysis. All geospatial processing was done in ArcGIS Desktop version 10.7 (Esri: Redlands, California).

2.3. Participant selection and meditation workshop

Novice and experienced healthy meditators and non-meditator controls were recruited, following informed consent, from three meditation retreats held within the United States (n = 117, 6 did not complete all biological collections and were excluded from the study). A total of 45 novice and 43 experienced meditators as well as 23 controls completed all study requirements and were included in the molecular studies. All experimental protocols were housed at VitaMed Research (Palm Desert, CA) and approved by the Western Institutional Review Board (WIRB; now WCG-IRB). All clinical records related to these studies are housed at VitaMed Research as mandated by federal laws. Research subject recruitment was random after a basic questionnaire set was utilized to determine eligibility criteria. The only inclusion criteria were having a current meditation practice incorporating the guided specialized meditation practice used at the retreats, being over 21 years of age, and in generally good health. Experienced meditators were identified as having followed this guided specialized meditation practice for more than 6 months and having attended a previous 7-day meditation retreat; novice meditators were identified as having followed the technique for less than 6 months and having not attended a previous retreat; control subjects were identified as having no meditation experience using this particular meditation practice and were vacationing guests traveling with workshop participants. The 7-day advanced meditation retreat consisted of approximately 25 h of instruction and 35 h of meditation focused around Kundilini techniques and containing elements of focused attention, non-dual awareness, and loving kindness/compassion meditation with a significant breathwork component. Meditations were carried out seated, standing, lying down, and/or walking. All subjects maintained a similar routine and time schedule and ate similar breakfasts and lunches during the week. To ensure scientific rigor and reproducibility, male and female subjects were used throughout these studies.

2.4. Human plasma collection

Meditation blood plasma samples were collected at Indian Wells 02/2020, Orlando 04/2021, and Denver 7/2021 retreats. All study subjects fasted for at least 30 min prior to providing a blood sample. In total, 23 controls, 45 novice, and 43 experienced meditators completed all biological collections and were included in the analyses. Blood was collected beginning at 12 p.m. and ending at 4 p.m. local time on retreat Days 0 and 1 (pre-retreat samples) and on Days 7 and 8 (post-retreat samples). All blood samples were stored at 4 °C (on wet ice) for no more than 1 h after collection. Plasma was isolated by centrifugation at 3000 RPM for 15 min using an E8 Touch tabletop centrifuge, aliquoted into 1.5 ml Eppendorf tubes, and immediately frozen on dry ice. All samples were stored and shipped to UC San Diego on dry ice.

2.5. Cell culture

Human lung epithelial cells line (A-549, ATCC© CCL-185) were maintained in culture in F–12K supplemented media (10% FBS, 1% Pen/Strep) at 37 °C, 5% CO_2. Cells were maintained at passages 3–8 for all experiments. For virus infection assays, 50,000 cells/well were cultured in 96 well plates. For microscopy, 50,000 cells were plated in poly-D-lysin-coated glass-bottom 35 mm dishes. Mouse skeletal muscle cells (C2C12, ATCC© CRL-1772) were used as a control cell line for viral infection assays. Cells were maintained in DMEM supplemented media (10% FBS, 1% Pen/Strep) at 37 °C, 5% CO_2.

2.6. Viral constructs

Viral constructs were prepared at the UCSD Vector Development Core Lab as described in Fig. 2a. Briefly, HIV-1 viral constructs were engineered to express red fluorescence protein under the control of the pCMV promoter. HIV-1 packaging plasmids were used in combination with the viral envelope proteins and including the SARS-CoV-2. Spike**Δ**19 protein. The same procedure was used to prepare the variants of SARS-CoV-2, including the Delta (B.1.617.2; HIV1.RFPCoV-2-S-Delta), Beta (B.1351; HIV1.RFPCoV-2-S-Beta), U.K. (B.1.1.7; HIV1.RFPCoV-2-S-UK), Brazil (P.1; HIV1.RFPCoV-2-S-Brazil), and D614G (Wuhan-Hu-1 D614G; HIV1.RFPCoV-2-S-D614G) variants.

2.7. Immunofluorescence assays

A-549 (or C2C12 control) cells were seeded in 35 mm glass bottom plates. After 24 h of culture, cells were treated with human plasma (1% final concentration in 2 mL culture media). After 1 h of treatment, 1×10^5 IU/mL of virus was added. Following 24 h of co-incubation, cells were treated with NucBlue™ LiveReadyProbes™ Reagents (Hoechst 33342) for nuclear staining and observed at 100X in a live cell imaging microscope (Keyence BZ-X700) coupled with an incubation chamber at 37 °C, 5% CO_2 and controlled humidity. All sample groups remained blinded until the completion of data analysis.

2.8. Scanning and transmission electron microscopy

Human lung epithelial cells were grown to confluence in six-well plates with or without glass coverslips. Cells were fixed with 2.5% glutaraldehyde, 4% paraformaldehyde in 0.1 M cacodylate buffer. For SEM analyses, coverslips were washed with 0.1 M cacodylate buffer, post-fixed with 1% OsO_4, dehydrated, and dried overnight with hexamethyl-D-silazane (HMDS). Coverslips were mounted and coated with 6 nm platinum before viewing on an FEI Quanta 450 FEG SEM. For TEM analyses, plates were washed with 0.1 M cacodylate buffer, post-fixed with 1% OsO_4, en-bloc stained with 1% uranyl acetate, followed by dehydration and embedding in LX112 (Ladd Scientific). Monolayers were sectioned on a Leica UC6 ultramicrotome, counterstained with uranyl acetate and lead, and viewed on an FEI Tecnai T12 TEM. To ensure scientific rigor and reproducibility, all groups remained blinded until the completion of data analysis.

2.9. Heat inactivation and ultracentrifugation of meditation plasma

A 500 μL aliquot of human plasma for pre- and post-meditation conditions was thawed. For each treatment, a 100 μL sample was used. Heat inactivation was carried out by incubation of the samples in a water bath for 1 h at 60 °C. Ultracentrifugation of the samples was performed at 100,000×*g* for 2 h at 4 °C in a Beckman benchtop Optima MAX-XP ultracentrifuge. Supernatants were collected, and pellets were resuspended in 100 μL of sterile 1X PBS.

2.10. Virus infection fluorescence studies

To quantify the effect of human plasma samples from meditators, 50,000 A-549 cells per well were seeded in 96-well plates. After 24 h in culture, cells were treated with human plasma (1% final concentration in 2 mL culture media). After 1 h of treatment, 1×10^4 IU/mL of virus was added. After 24 h of co-treatment, RFP fluorescence was measured in a TECAN Spark® plate reader, followed by nuclear staining with NucBlue™ LiveReadyProbes™ Reagents (Hoechst 33342) and subsequent DAPI fluorescence measurement. To determine the effect of SERPINA5 on infection by different SARS-CoV-2 variants, cells were pre-treated for 1 h with 0.75 ng/μL of recombinant SERPINA5 (Abcam, ab229370), followed by 1×10^4 IU/mL of virus. Fluorescence measurements were performed after 24 h. Data is presented as RFP-relative

fluorescence normalized by DAPI-relative fluorescence. To ensure scientific rigor and reproducibility, all experimental groups remained blinded until the completion of data analysis.

2.11. Co-immunoprecipitation of plasma proteins with SARS-CoV-2. SΔ19-RFP

Human plasma (100 μL) was incubated with 2.5×10^5 IU/mL of SARS-CoV-2.SΔ19-RFP for 1 h with constant rotation at 37 °C. Samples were subjected to immunoprecipitation using magnetic beads conjugated with Anti-SARS Spike antibody (Abcam, ab273433), following Pierce™ Crosslink Magnetic IP/Co-IP Kit manufacturer's instructions. Proteomics analysis was used to determine all proteins that interacted with the viral particles. All sample groups remained blinded until the completion of data analysis.

2.12. Proteomics sample preparation

Proteins eluted from co-IP experiments were processed using S-trap micro columns (Protifi, NY, USA) following the manufacturer's protocol. Briefly, samples were diluted to twice their original volume using 10% SDS, 100 mM TEAB buffer pH 8.5. Disulfide bond reduction was carried out using 5 mM dithiothreitol (DTT) at 56 °C for 30 min. Methylation of broken disulfide bonds was done using 15 mM iodoacetamide (IAA) in a darkened environment for 20 min. The methylation reaction was quenched using 5 mM DTT, followed by incubation of samples in a darkened environment for 15 min. Phosphoric acid (2.5% final concentration) was added for pH adjustment (pH $\leq$ 1). The reaction was diluted 6-fold using binding buffer (100 mM TEAB, 90% methanol). This mixture was then loaded onto an S-trap microcolumn and centrifuged at 4000×*g* for 30 s. Each column was washed 5X with binding buffer. All protein was digested (digestion buffer, 1 μg trypsin in 50 mM TEAB) at 47 °C for 3 h and eluted using 50 mM TEAB followed by 0.2% formic acid and 50% acetonitrile. The peptides were desalted on a C18 resin column and dried under vacuum. Samples were resuspended in 50 μL of resuspension buffer (30% dry acetonitrile and 50 mM HEPES, pH 8.5). An internal standard (bridge channel) was prepared from the peptide by mixing 5 μL of each sample together and separating aliquots of 45 μL from this mixture for each 10-plex. TMT reagents were resuspended by vortex mixing for 5 min in resuspension buffer. Labeling was performed on resuspended peptides by mixing peptides with TMT reagent for 1 h at room temperature. Reactions were quenched with 9 μl of 5% hydroxylamine followed by incubation for 15 min at room temperature. After reaction quenching, samples were acidified using 50 μL of 1% TFA. Bridge channels for the proteomics experiment were assigned to the 131 TMT label for all 10-plexed runs. Following acidification of labeled samples, labeled peptides within each 10-plex were mixed, desalted on C18 resin columns, and lyophilized.

2.13. Liquid chromatography-"tribrid" MS (LC-MS/MS/MS)

Dried fractions were resuspended in a solution of 5% acetonitrile and 5% formic acid. Mass spectrometry-based proteomic data collection was performed using an Orbitrap Fusion mass spectrometer with an in-line Easy nano-LC. Each 10-plex was run on 3 h gradients. The gradient ranged from 3% acetonitrile, 0.125% formic acid to 100% acetonitrile, 0.125% formic acid over each run. Peptides were separated using an in-house-prepared column with a length of 30 cm, inner diameter of 100 μm, and outer diameter of 360 μm. The column was packed at the front end with 0.5 cm of C4 resin (5 μm particle size) and 0.5 cm of C18 resin (3 μm particle size). The remainder of the column was packed with C18 resin (1.8 μm particle size). Ionization at the source was facilitated by applying 2 kV of electricity through a T-junction connecting sample, waste, and column capillary lines.

MS spectrum acquisition was performed in data-dependent mode with a survey scan range of 500 to 1200 m/z and a resolution of 60,000. Automatic gain control (AGC) was set to 2×10^5, and the maximum ion inject time was 100 ms. Synchronous precursor selection was used for MS2 and MS3 analysis. MS2 data were collected with the decision tree tool. The settings for the decision tree were as follows. Ions with 2 charges were analyzed at between 600 and 1200 m/z, while ions with 3 or 4 charges were analyzed at between 500 and 1200 m/z. The lower ion intensity threshold was 5×10^4. Selected ions were isolated in the quadrupole at 0.5 Th and fragmented with collision-induced dissociation (CID). Fragment ions were detected in the linear ion trap with a high-scan-rate AGC setting of 1×10^4. Data were then subjected to centroid analysis.

Fragmentation of TMT reporter ions was performed at the MS3 stage using synchronous precursor selection. The 10 precursors chosen at the MS2 stage were fragmented using high-energy collisional dissociation (HCD) fragmentation. Reporter ion detection occurred in the Orbitrap mass spectrometer with a resolution of 60,000 and the lower detection limit set at 110 m/z. AGC at this stage was 1×10^5, and the maximum injection time was 100 m. Data were then subjected to centroid analysis. Precursor ions 40 m/z below and 15 m/z above the MS2 m/z value were then jettisoned.

2.14. Mass spectra data processing, normalization, and availability

Spectral matching and filtering were performed using Proteome Discoverer 2.1 software (Thermo Fisher Scientific, USA). Spectral matching was performed using the Uniprot Homo sapiens reference proteome downloaded on 2 July 2018. For proteomic analysis, the SEQUEST algorithm was used for decoy database generation. Precursor ion mass tolerance was set to 50 ppm, and fragment ion mass tolerance was 0.6 Da. The enzyme was set as trypsin, and two missed cleavages were allowed. The peptide length range was 6–144 amino acids. One dynamic modification was used, methionine oxidation (+15.995 Da). Static modifications included isobaric tandem mass tags at the N termini and on lysine residues (+229.163 Da) and carbamidomethylation of cysteines (+57.021 Da). Filtering of spectra was performed in Percolator at the peptide and protein levels against the previously generated decoy database. Following search completion, data were filtered for high peptide spectral match (PSM) confidence and PSM disambiguity/selection. For proteomics, filtered PSM quant data were summed to the protein level. Data were normalized against the bridge channel values for each protein divided by the median of all bridge channel values. A second normalization step was performed by normalizing the average-normalized values against the median values for each TMT channel divided by the median of all TMT channel medians. Data processing and volcano plot generation were done using R and Python. Raw mass spectrometry data can be found in the MassIVe spectral repository and are available at ProteomeXchange. To ensure scientific rigor and reproducibility, all groups remained blinded until the completion of data analysis.

2.15. SERPINA5 ELISA

To determine the concentration of SERPINA5 in the blood plasma of meditators, 100 μL of sample was used for each well of a SERPINA5 (human) ELISA kit (Abnova, KA5307), following the manufacturer's instructions. To determine the concentration of SERPINA5 in the plasma of vaccinated, non-meditators, a separate set of blood samples was collected in February of 2022 during a 14-day window from a group of non-meditators (n = 16) that had received two doses of BNT162b2 (Pfizer-BioNtech) or mRNA-1273 (Moderna) mRNA vaccines as well as a single booster dose. These samples were also used for the pseudovirus infection assays.

2.16. Molecular modeling studies

To assess the relatedness of SERPINs, sequences were input into

Geneious 11.1.5, and alignments of related α-SERPINs were completed using the Geneious multiple alignment tool. SERPINA5 (PDB 2OL2) was aligned with SERPINA1 (PDB 3CWM) using the RCSB pairwise structural alignment tool. The jFATCAT-rigid algorithm was used for the alignment. Results from the alignment were presented, including the RMSD, TM-Score, sequence identity and similarity, as well as the length of the proteins. For docking studies, molecular structures obtained from PDB TMPRSS2 (PDB 7MEQ) and SERPINA5 (PDB 2OL2) were uploaded to the ClusPro (Comeau et al., 2004) and FireDock (Mashiach et al., 2008) tools to assess potential protein-protein docking solutions. FireDock is a tool for refining and re-scoring protein-protein docking solutions. ClusPro provides ranked solutions-based global energy. The best solution was determined by the algorithm and presented as a possible solution.

2.17. Statistical analysis

To determine relative fluorescence intensity differences between pre- and post-meditation samples, a paired analysis was performed for each experimental group (two-tailed, Mann-Whitney post-test; *P < 0.05). Human SARS-CoV-2 Spike (trimer) IgM antibody levels in post-meditation samples were compared by one-way Anova with Tukey's post-test (*P < 0.05). Correlation between human SARS-CoV-2 Spike (trimer) IgM antibody levels and SARS-CoV2.SpikeΔ19-RFP infection protection (post-meditation relative fluorescence intensity, RFP/DAPI) was analyzed by Pearson's correlation. To ensure scientific rigor and reproducibility, all experimental groups remained blinded until the completion of data analysis. Based on n = 23 controls, n = 45 novice meditators, and n = 43 experienced meditators, using α = 0.05 and power = 0.80 for a two-tailed Mann-Whitney post-test, we have the power to detect effect sizes as small as d = 0.8654 for controls, d = 0.6114 for novice meditators, and d = 0.6258 for experienced meditators.

3. Results

3.1. Responses from participant survey indicate that length and frequency of meditation practice improve management of COVID-19

We carried out a survey sent to a total of 22,459 individuals that had attended a 7-day meditation workshop. A total of 2844 respondents completed the survey, coming from 66 countries, as well as 49 states within the United States (US), with the sample being predominantly female (80.0%), Caucasian (70.4%), and having a notable proportion with a history of smoking (26.5%; Supplementary Table S1). Furthermore, 64.8% of respondents were from the US and 28.3% of the US sample were residents of either California (n = 304) or Florida (n = 218), the most represented US states. Sixty-three geospatial units with at least the minimum sample size (n = 10) were analyzed, with 17 countries (excluding the US), 31 US states (excluding California and Florida), and 15 counties from California or Florida. In bivariate regression analysis, the proportion of communities with respondents having at least six months of meditation experience (i.e., experienced meditators) was significantly associated with reduced COVID-19 infection (β = -0.307, $p < 0.001$; Fig. 1a).

Importantly, among those having been infected with SARS-CoV-2 virus (n = 372; 13.1%), rate of brain fog (β = −0.621, $p = 0.001$; Fig. 1b) and rate of congestion (β = −0.565, $p = 0.001$; Fig. 1c) were significantly reduced in experienced meditators. There was also a trend towards reduced duration of illness (β = −0.895, $p < 0.080$; Fig. 1d) in experienced meditators. Further, those that meditated daily showed a significantly reduced rate of anosmia (β = −0.756, $p = 0.025$; Fig. 1e) among those with COVID-19. In subject-level bivariate analyses, SARS-CoV-2 infection was significantly inversely associated with both meditation frequency (OR = 0.212, $p < 0.001$; Fig. 1f) and meditation experience (OR = 0.251, $p < 0.001$; Fig. 1g). Among those having had COVID-19, less meditation experience also significantly predicted brain fog (OR = 0.115, $p < 0.001$; Fig. 1h) and COVID-19 duration (β = −0.081, $p < 0.001$; Fig. 1i). Measures of fit (R^2 for linear models and Nagelkerke's R^2 for logistic models) did not exceed 0.02 in subject-level bivariate analysis. However, backwards selection revealed multivariable models explaining greater variability in SARS-CoV-2 infection (Nagelkerke $R^2 = 0.039$; Supplementary Table S2; Fig. 1j), brain fog (Nagelkerke $R^2 = 0.092$; Supplementary Table S2; Fig. 1k), and COVID-19 duration ($R^2 = 0.098$; Supplementary Table S2; Fig. 1l). For all of these multivariable models, the backward selection algorithm selected meditation experience as a significant predictor as well as a racial/ethnic covariate. Additional analysis was performed to investigate the role of vaccination status on COVID-19 risk. Respondents who had been vaccinated were significantly less likely to be infected with COVID-19 (β = −0.038, $p = 0.005$; Fig. 1m). In a multivariable model with both vaccination status and meditation experience, both terms retained statistical significance (respectively, $p = 0.005$ and $p < 0.001$; Fig. 1n). Taken together, these data suggest that length of meditation practice may influence susceptibility and management of COVID-19, even after controlling for health disparities and other behaviors.

3.2. Blood plasma from experienced meditators limits entry of pseudotyped SARS-CoV-2 virus

At three 7-day advanced meditation retreats held in February 2020 and in April and July of 2021, we collected blood plasma from novice and experienced meditators. Blood plasma was also collected from "vacation" control subjects not participating in the workshop but staying at the retreat venue. Blood sample collection was carried out at two timepoints, one before (pre) and one after (post) the meditation retreat. We generated pseudotyped virus using lentiviral constructs and the envelope-expressing SARS-CoV-2 spike protein (Fig. 2a). The core was packed with a red fluorescent protein (RFP) reporter and transmission electron microscopy (TEM) showed structural similarity to coronavirus (Fig. 2a). As SARS-CoV-2 is selective to human infection, we tested infectivity in human (A-549) vs. rodent (C2C12) cells. We observed selective infection of SARS-CoV-2 pseudovirus in human lung epithelial cells (Fig. 2b). We next developed a screening assay to test the effect of blood plasma in adoptive transfer experiments. While addition of virus resulted in an increase in RFP signal in the positive control, RFP signal was diminished in A-549 cells incubated with plasma from experienced meditators following the 7-day advanced workshop (Fig. 2c). We performed scanning electron microscopy (SEM) and TEM to visualize qualitative localization of pseudovirus after adoptive blood plasma transfer. SEM revealed that the majority of the virus in the experienced and novice plasma-treated cells was trapped on the cell surface, while the surface of the control plasma-treated cells was clear (Fig. 2d). TEM analysis revealed abundant intracellular viral particles in control plasma-treated samples, less in the novice, and little in the experienced (Fig. 2d). Next, we developed a plate reader-based assay to measure red fluorescence signal. We observed a significant reduction in RFP signal in cells treated with post-meditation plasma from novice and experienced, but not control subjects (Fig. 2e). This reduction in RFP signal was not dependent on sex, as plasma from male and female meditators show a robust effect (Fig. 2f and g). Next, we explored an age-specific effect of post-meditation plasma (Fig. 2h). Interestingly, we see a negative correlation in the pre-to post-difference change in control and novice groups, suggesting a slight (though insignificant) increase in RFP signal with age. Interestingly, we observed a slight positive correlation in experienced post-meditation plasma with age. Taken together, these data suggest that there is no effect of sex and a minimal effect of age on the dynamics of meditation and *in vitro* pseudovirus infection.

To determine the nature of the factors responsible for these observations, we subjected the plasma to heat inactivation (Fig. 2i) and high-speed centrifugation followed by treatment of cells with supernatant (Fig. 2j) or solubilized pellet (Fig. 2k).

Protection was abrogated following heat denaturation and not

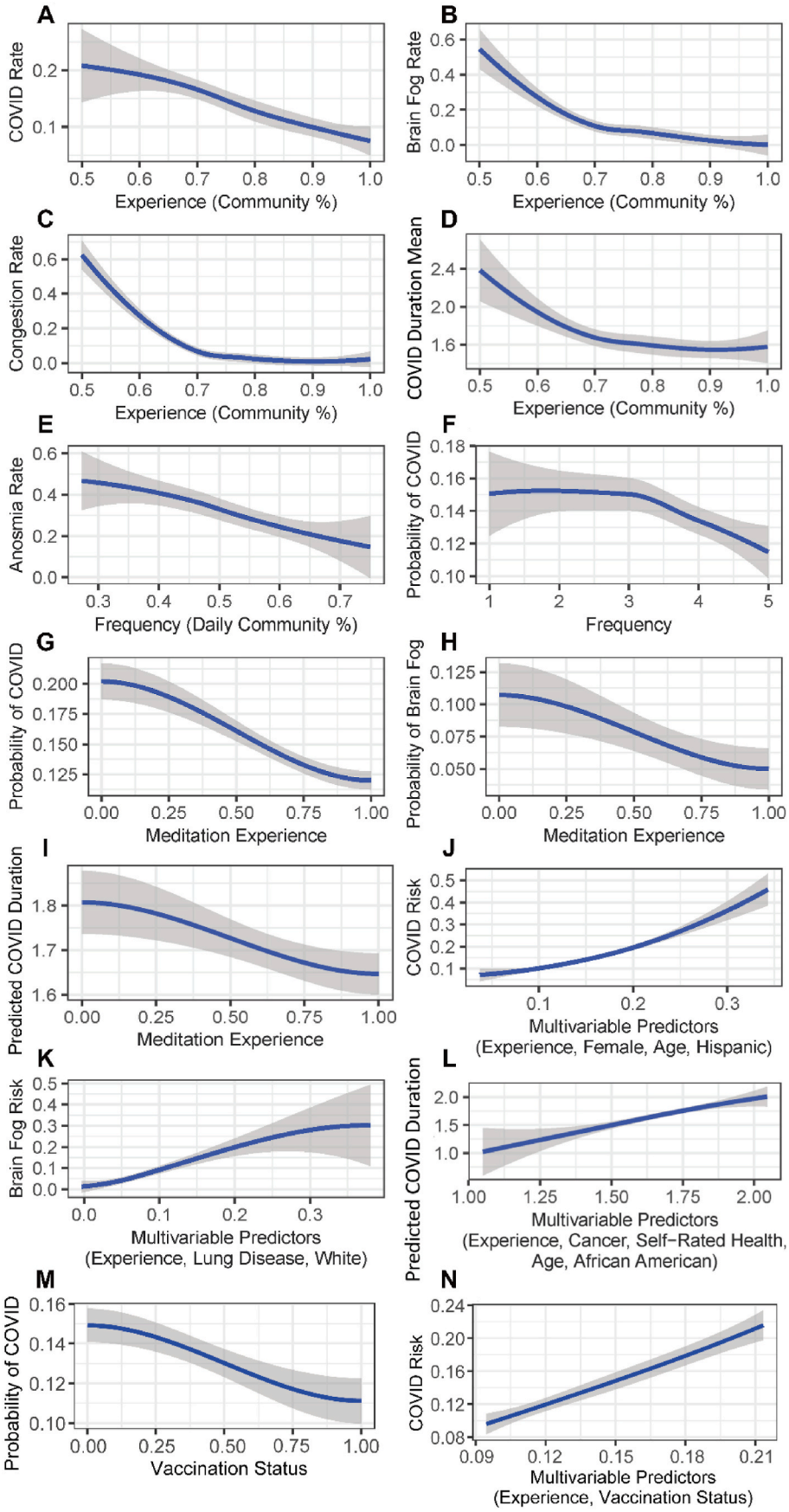

Fig. 1. Graphical representation of meditator survey data. a-d, Among lowest-resolution geospatial communities meeting a minimum sample size of 10, relationships between the proportion of participants from a 7-day meditation workshop having at least six months of meditation experience and their self-reported rates of COVID-19 infection **(a)**, brain fog **(b)**, congestion **(c)**, and duration of illness **(d)**. **e,** Relationship between the proportion of participants from a 7-day meditation workshop, grouped by geospatial area, that meditates daily and rate of anosmia. **f,** Among individual respondents, the relationship between meditation frequency and probability of COVID-19 infection. **g-i,** Among individual respondents, the relationship between meditation experience (binary; six months of experience) and COVID-19 infection **(g)**, brain fog **(h)**, and duration of illness **(i)**. **j-l,** Among individual respondents, the relationship of multivariable predictors selected by backwards selection (Wald $\chi 2$) and COVID-19 infection **(j)**, brain fog **(k)**, and duration of illness **(l)**. **m,** Among individual respondents, relationship between the probability of COVID-19 and vaccination status. **n,** Among individual respondents, the relationship of multivariable predictors and COVID-19 infection. All regression curves were plotted with LOESS (span $\alpha = 1.50$).

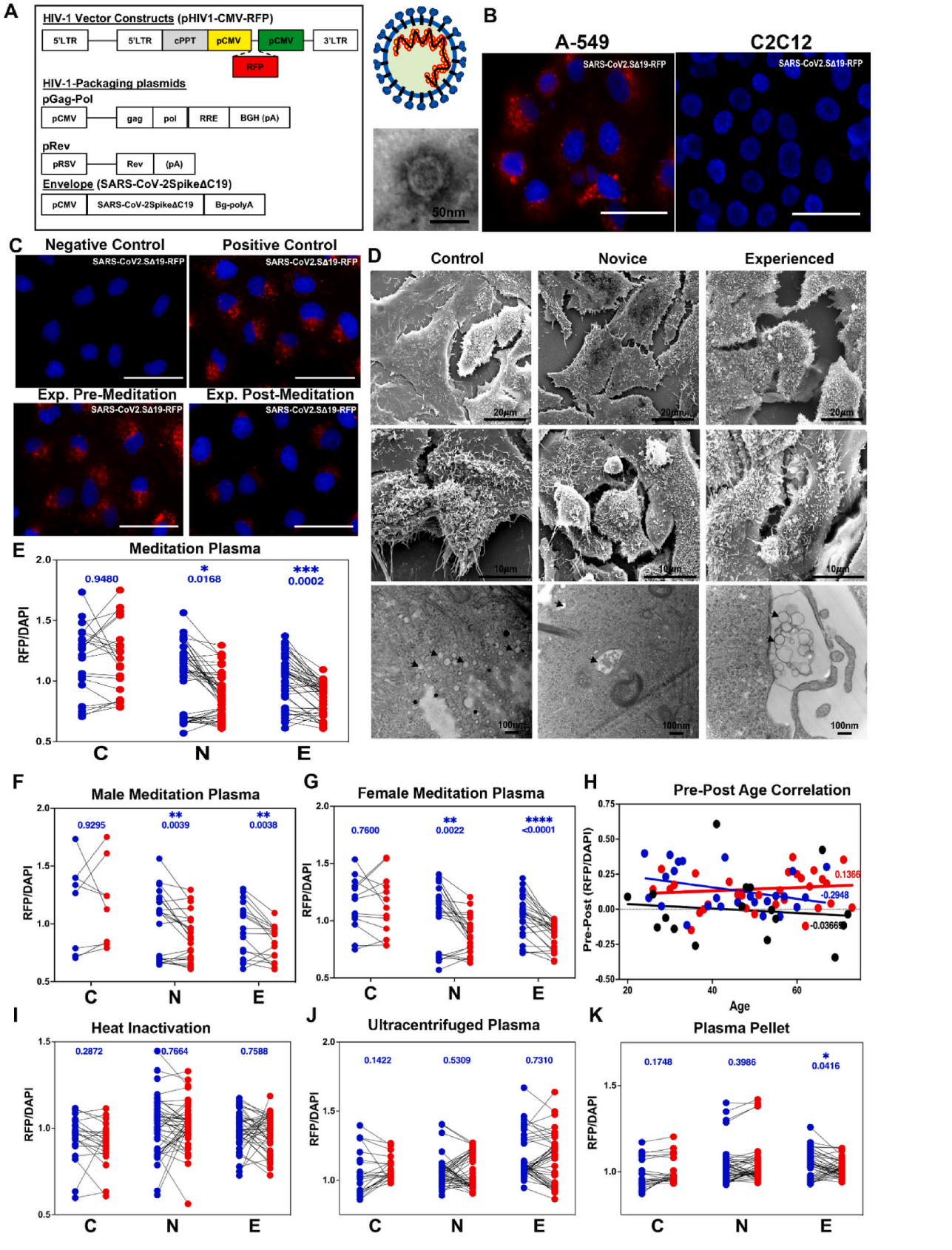

(caption on next page)

Fig. 2. Meditation induces the expression of bloodborne factors that protect against SARS-CoV-2 infection. a, Schematic representation of SARS-CoV-2.SD19-RFP pseudovirus construction and transmission electron microscopy (TEM) image of virion. **b,** Human lung cells (A-549) and mouse muscle cells (C2C12) 24 h after exposure to SARS-CoV-2.SD19-RFP. **c,** Representative immunofluorescence images of A549 cells 24 h after exposure to pseudovirus. Negative control represents vehicle only while positive control cells were exposed to pseudovirus (upper panels). Lower panels represent cells pre-treated with either experienced pre- (left panel) or post- (right panel) meditation plasma prior to addition of pseudovirus. Red, red fluorescent protein (RFP); Blue, Hoechst 33342. Scale bars, 50 μm **d,** Scanning EM (SEM) (upper and middle panels) and TEM (lower panels) images of A549 cells treated with post-meditation plasma from control, novice, or experienced meditators, followed by addition of pseudovirus. **e,** Quantification of red fluorescence intensity in A549 cells treated with control, novice, or experienced pre- and post-meditation plasma followed by addition of pseudovirus. Two-tailed analysis, Mann-Whitney post-test (control $n= 21$, novice $n= 45$, experienced $n= 43$) was performed ($^*p < 0.05$). **f-g,** Correlation of sex with red fluorescence intensity in A549 cells treated with control, novice, or experienced pre- and post-meditation male **(f)** and female **(g)** plasma followed by addition of pseudovirus. Two-tailed analysis, Mann-Whitney post-test (control $n= 8$ *male*, 13 female; novice $n= 23$ *male*, 22 female; experienced $n= 17$ *male, 26 female*) was performed ($^*p < 0.05$). **h,** Pre-post correlation of red fluorescence intensity with age in A549 cells treated with control, novice, or experienced meditation plasma. A positive pre-post value is indicative of a positive correlation of age and protection from pseudoviral infectivity, while a negative pre-post value demonstrates a negative correlation. Two-tailed analysis, Mann-Whitney post-test (control $n= 20$, novice $n= 44$, experienced $n= 43$) was performed ($^*p < 0.05$). **i-k,** A549 cells were pre-treated with heat-inactivated **(i)** or ultra-centrifuged plasma supernatant **(j)** or pellet **(k)** from control, novice, or experienced meditators pre- and post-meditation, followed by addition of pseudovirus. Cells were fixed and stained 24 h after addition of pseudovirus. Two-tailed analysis, Mann-Whitney post-test was performed ($^*p < 0.05$). Blue dots, pre-meditation; red dots, post-meditation. (For interpretation of the references to color in this figure legend, the reader is referred to the Web version of this article.)

present in the supernatant following high-speed centrifugation. However, protection was retained in the solubilized pellet, strongly suggesting that the protective factor is a protein and may be membrane-associated or within a membrane-bound, vesicular compartment. It is important to note that blood collection on the majority of meditation subjects occurred at a time before the COVID-19 vaccines became widely available.

3.3. *SERPINA5 as a possible factor elevated in meditators and responsible for limiting SARS-CoV-2 infection*

To identify candidate proteins that limit viral infection, we performed immunoprecipitation experiments using SARS-CoV-2 spike protein antibodies incubated with meditator plasma and pseudovirus. Mass spectroscopy revealed several proteins in the interactome with the pseudovirus. One of these proteins, SERPINA5, is a protease inhibitor that belongs to a large superfamily of proteins (Kelly-Robinson et al., 2021) important in immune modulation (Wojta, 2020). Due to its biological function and high prevalence in the experienced vs. control group (Fig. 3a), SERPINA5 was identified as a possible protein of interest and became the focus of these studies. To assess any differences in plasma SERPINA5 levels between control and meditator groups, we performed ELISA analysis on post-meditation plasma from control subjects and experienced meditators (Fig. 3b). This analysis revealed significantly higher SERPINA5 levels in post-meditation plasma from experienced meditators relative to control subjects. To determine whether vaccination leads to a rise in plasma SERPINA5, we included plasma from non-meditators vaccinated and boosted with either BNT162b2 (Pfizer-BioNTech) or mRNA-1273 (Moderna) mRNA-based vaccines. As shown in Fig. 3b, SERPINA5 is not elevated following SARS-CoV-2 vaccination and is similar to that present in control plasma.

Next, we rationalized that SERPINA5 may target transmembrane protease, serine 2 (TMPRSS2), a major protease involved in SARS-CoV-2 entry. This hypothesis could not be directly tested with the meditation plasma samples due to incompatibility of plasma with the TMPRSS2 assay kit. Given the importance of TMPRSS2 in SARS-CoV-2 viral entry, one might predict that plasma samples with a higher concentration of SERPINA5 would be associated with lower levels of infectivity, resulting in a lower RFP fluorescence signal. As shown in Fig. 3c, we observed an inverse correlation between plasma SERPINA5 and RFP fluorescence. These data suggest that SERPINA5 in experienced meditator plasma leads to protection from viral infectivity, providing indirect support for a role as a TMPRSS2 inhibitor. Previous studies on SERPINA1 (alpha-1-antitrypsin (A1AT)) have demonstrated that it can potently inhibit TMPRSS2 at physiologic concentrations in HEK293T cells engineered to overexpress the protease (Azouz et al., 2021) and in primary human airway cells (Wettstein et al., 2021). To determine the level of structural similarity between SERPINA1 and SERPINA5, we carried out molecular modeling studies using a structural alignment algorithm to generate a 3D structural model of the proteins superimposed on one another (Fig. 3d). Structure alignment is useful to compare proteins that may be related or have similar functions based on evolutionary relationships. The metrics for this analysis indicate a high level of structural similarity between the proteins. Taken together, these data support the hypothesis that SERPINA5 can serve as an inhibitor of TMPRSS2.

To further explore the possibility that SERPINA5 can bind to and inhibit TMPRSS2, we carried out molecular modeling studies using the known protein structures of TMPRSS2 catalytic domain and SERPINA5. Shown in Fig. 3e are ribbon diagrams for the catalytic domain of TMPRSS2 (left panel), SERPINA5 with reactive center loop (middle panel), and bound uncleaved (bottom right panel) and cleaved (bottom top panel) forms of SERPINA5, the latter resulting in covalent inhibition characteristic of SERPIN family members. The energetic parameters obtained, including a Firedock global energy of 3.21, an attractive Van der Wal (VdW) of −1.35, a repulsive VdW of 0.49, an ACE of −0.46, and an HB of 0.0, represent the most energetically favorable docking structure.

3.4. *Plasma from experienced meditators differentially protects against key SARS-CoV-2 variants*

The emergence of new variants of the original SARS-CoV-2 virus strain has been a constant challenge since the beginning of the pandemic (Raman et al., 2021). The increased levels of SERPINA5 in meditators represent a potential biological strategy against other variants. When A-549 cells were challenged with SARS-CoV-2 pseudovirus variants (Fig. 4a–f), we observed a significant protective effect against the Delta (B.1.617.2 lineage) and D614G (novice meditators only) variants, with no protection against Lambda (C.37), Beta (B.1351), U.K. (Alpha; B.1.1.7), and Brazil (Gamma; P.1 and descent) variants. To further explore the relationship between plasma SERPINA5 and protection from infectivity in experienced meditators, we examined the relationship between high SERPINA5 levels (500 pg/mL or higher) and RFP fluorescence. With the exception of the Delta variant, there was no correlation between high plasma SERPINA5 and protection from infection with the SARS-CoV-2 variants analyzed. These data demonstrate a differential effect of SERPINA5 relative to unique mutations of the viral spike protein and suggest that, with the exception of Delta, these variants may not rely on TMPRSS2 for viral entry and likely use other mechanisms.

Recently, the BNT162b2 vaccine (Pfizer-BioNTech) has been shown to be less effective in preventing infection with the Delta variant when compared with the U.K. (Alpha) variant (Eyre et al., 2022), consistent with previous studies demonstrating compromised efficacy of the Delta variant (Mlcochova et al., 2021). In a separate study, Jalkanen and colleagues have explored the effects of this vaccine on antibody

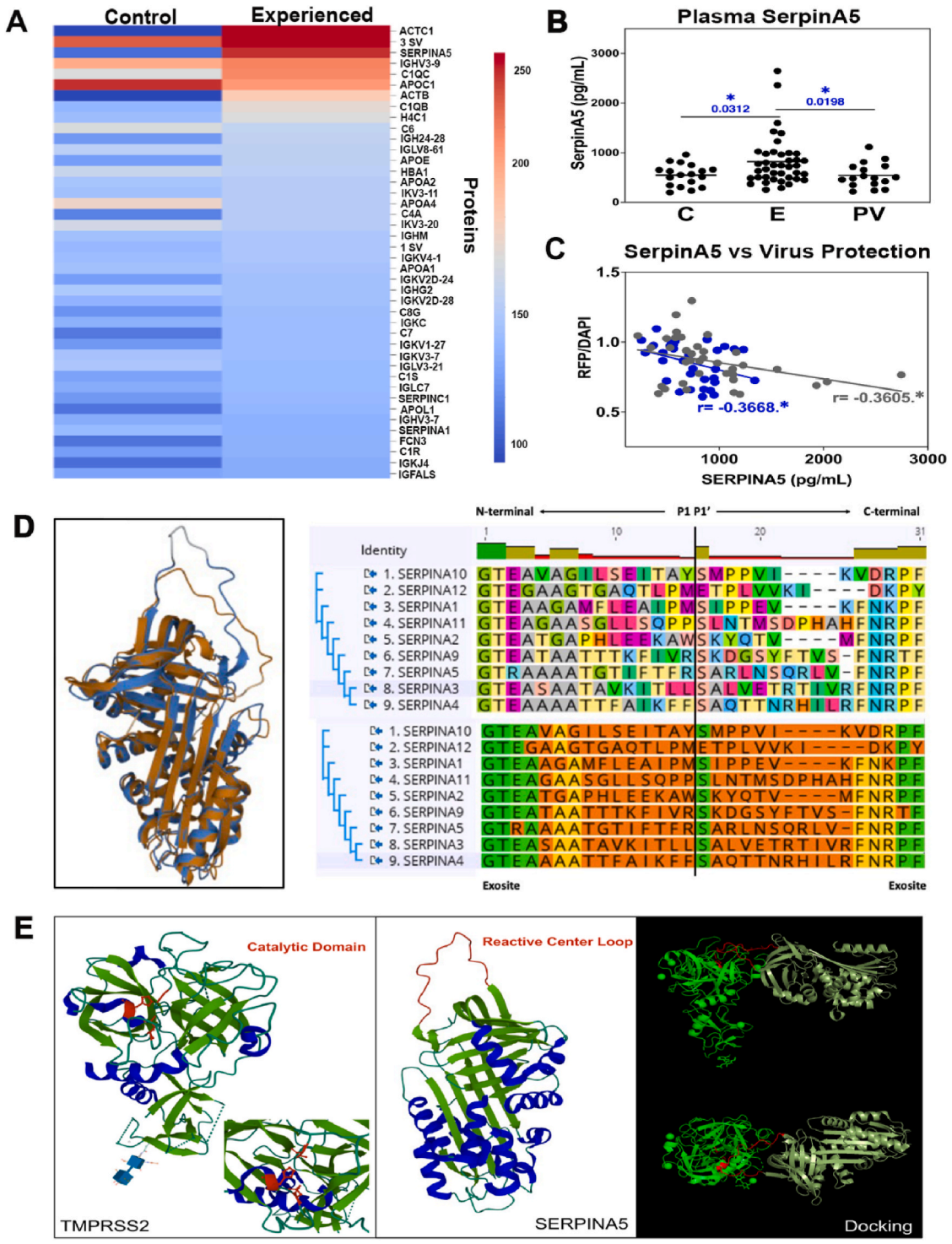

Fig. 3. Experienced meditators have elevated levels of plasma SERPINA5. a, Pseudovirus interactome co-immunoprecipitated from control and experienced post-meditation plasma using spike antibody. **b,** SERPINA5 concentration (pg/mL) in control and experienced post-meditation plasma (control *n=18*, experienced *n=40*). **c,** Correlation analysis between plasma SERPINA5 concentration (pg/mL) and viral infection protection (RFP/DAPI) in novice (n = 37, gray dots) and experienced (n = 33, blue dots) meditators. r, Pearson's correlation value, (*$p < 0.05$). **d,** Ribbon diagram of SERPINA1 (3CWM) and SERPINA5 (2OL2) superimposed on one another. SERPINA1 and SERPINA5 were aligned with the RCSB pairwise structure alignment tool (Berman et al., 2000) using the iFACTCAT(rigid) algorithm (Li et al., 2020). The reactive center loop (RCL) is depicted in the right panel for all inhibitory clade A SERPINs. The top alignment represents color by amino acid while the bottom alignment represents similarity as calculated by Blosum62 score matrix in Geneious (G. 11.1.5). Green amino acids represent 80–100% similarity, yellow amino acids represent 60–80% similarity, and orange amino acids represent less than 60% similarity. Both N- and C-terminal exocites are intact as well as a central Ser (P1|P1') with the exception of SERPINA12. Alignment scheme adapted from Sanrattana et al. (Sanrattana et al., 2019). **e,** Ribbon diagrams of TMPRSS2 (PDB 7MEQ) (catalytic domain, depicted in red; left panel), SERPINA5 (2OL2) with RCL (depicted in red; middle panel). Beta sheets are shown in green, α-helices in blue. Potential TMPRSS2/SERPINA5 docking structures are indicated (right panel). Firedock global energy (3.21), attractive VdW (−1.35), Repulsive VdW (0.49), ACE (−0.46), HB (0.0). (For interpretation of the references to color in this figure legend, the reader is referred to the Web version of this article.)

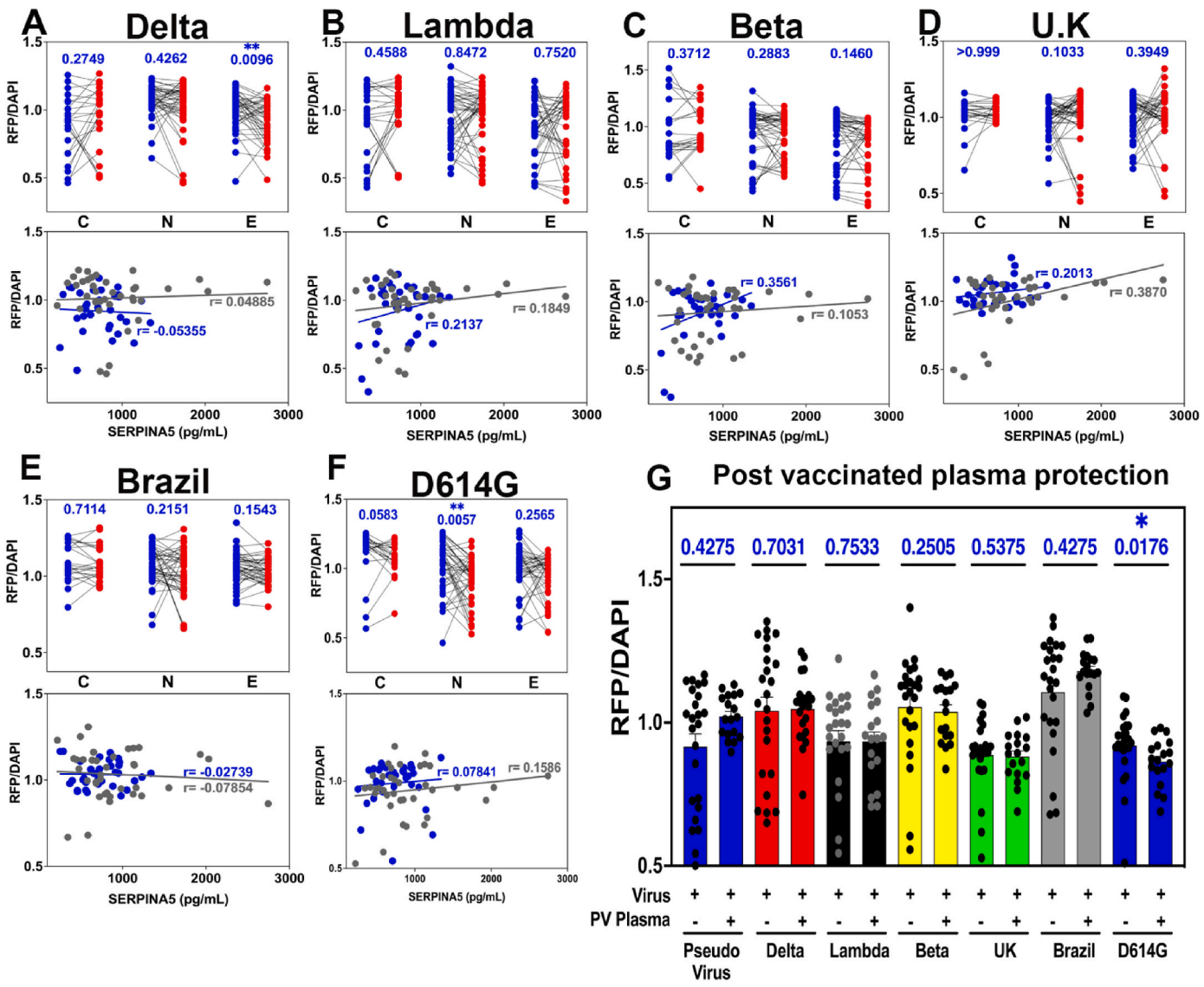

Fig. 4. Effect of post-meditation plasma, vaccination, and SERPINA5 on infectivity of SARS-CoV-2 virus variants. a-f (upper panels), Effect of plasma from control, novice, and experienced meditators on SARS-CoV-2 pseudovirus variant infectivity in A549 cells with Delta **(a)**, Lambda **(b)**, Beta **(c)**, U.K. **(d)**, Brazil **(e)**, or D614G **(f)** variants. Viral constructs were added to cultured cells following pre-treatment with control or meditation plasma. Two-tailed analysis, Mann-Whitney post-test (control $n= 23$, novice $n= 45$, experienced $n= 43$) was performed ($*p < 0.05$). **(lower panels),** Correlation analysis between plasma SERPINA5 concentration (pg/mL) and viral infection protection (RFP/DAPI) in novice (n = 37, gray dots) and experienced (n = 33, blue dots) meditators. r, Pearson's correlation value, ($*p < 0.05$). **g,** Effect of post-vaccination plasma on SARS-CoV-2 pseudovirus variant infectivity in A549 cells. Two-tailed analysis, Mann-Whitney post-test was performed ($*p < 0.05$). (For interpretation of the references to color in this figure legend, the reader is referred to the Web version of this article.)

responses against the U.K. (Alpha), Beta, and D614G variants and have shown the vaccine to have differential effectiveness to these different variants (Jalkanen et al., 2021). To investigate vaccine effects on SARS-CoV-2 variants using our pseudovirus infectivity assay, we pre-treated cells with plasma from post-vaccinated, non-meditators prior to the addition of pseudovirus. As shown in Fig. 4g, post-vaccination plasma was able to provide protection from infection with only the D614G variant, supporting previous findings (Eyre et al., 2022; Mlcochova et al., 2021; Jalkanen et al., 2021). These data demonstrate that while vaccination may reduce morbid COVID-19 disease (Pawlowski et al., 2021), it exhibits differential reactivity to the SARS-CoV-2 variants.

Based on our present findings, we propose a model for the biological effects induced by regular meditation practice. These effects involve changes that may include the expression of diverse plasma proteins, one being SERPINA5, an important molecule for regulating SARS-CoV-2 infection of the original strain of the virus as well as the Delta variant.

4. Discussion

Mind-body practices such as meditation have long been known to lead to a host of health benefits, including improvements in the stress response as well as immunity. Numerous studies carried out in recent years suggest that there is a correlation with length of meditation practice and improvements in physical and psychological health (Chang et al., 2011) along with corresponding improvements in the blood environment of practitioners (Bhasin et al., 2013; Epel et al., 2016). Here, we show a strong correlation between the length of meditation practice and the ability to limit COVID-19 disease and morbidity. Additionally, we show that meditation can lead to changes in the blood environment, including factors that afford protection against SARS-CoV-2 infection. We find one of these factors to be SERPINA5, a major player in coagulation and the immune response. Future studies will be aimed at further characterizing this meditation plasma for changes in gene expression and biomolecule composition, as well as the

ability to improve overall cellular immunity and function. These studies will provide insight into the molecular changes that arise from meditation and the role of meditation experience in this process.

SERPINs are highly abundant protein components of the blood, accounting for up to 10% of protein in circulation (Lucas et al., 2018). In addition, these proteins are the largest and most functionally diverse superfamily of protease inhibitors (Kelly-Robinson et al., 2021). The human genome encodes 37 *SERPIN* genes (Kelly-Robinson et al., 2021). Having a broad distribution pattern, SERPINs were initially identified for their role in regulating the thrombotic and fibrinolytic pathways via irreversible suicide inhibition of the serine proteases driving these pathways (Mkaouar et al., 2019). More recent studies have demonstrated that SERPINs can interact directly with and regulate immune cell responses and inflammation beyond direct effects on the coagulation cascades (Wojta, 2020). Given their strong inhibitory mechanisms, SERPINs are now being explored as therapeutics for a host of diseases, including cancer (McKee et al., 2012), lung disease (Lorincz and Curiel, 2020), Alzheimer's disease (Li et al., 2021), and autoimmune conditions such as lupus (Elshikha et al., 2016, 2018). Interestingly, a role for SERPINE1 in protection against the respiratory pathogen *Klebsiella pneumoniae* has been shown in a transgenic mouse model engineered to overexpress the protein. The authors demonstrated that these mice exhibited an enhanced immune response and were protected from sepsis and distal organ injury (Renckens et al., 2007). Along these lines, the increase in SERPIN expression observed following meditation would be consistent with an improvement in immunity and overall health.

More recent studies have shown that physiologic concentrations of SERPINA1 (A1AT) can suppress replication of SARS-CoV-2 in both cell lines as well as in primary human epithelial cultures (Wettstein et al., 2021). This highly abundant SERPIN was also shown to specifically bind and inactivate TMPRSS2, thus blocking viral entry (Wettstein et al., 2021). For these reasons, as well as a host of others, SERPINA1 has been hypothesized as a potential treatment option for COVID-19 (Bai et al., 2021). Our data suggest that SERPINA5 may play a significant role in protection from SARS-CoV-2 infection following an intensive meditation experience. A protective role for SERPINA5 in COVID-19 is evidenced by a large multi-omic study carried out on blood samples from 128 COVID-19-positive and -negative hospital patients with moderate to severe respiratory issues. This study revealed strong biomolecule associations with COVID-19 status and severity. Interestingly, the authors found a strong inverse correlation between COVID-19 severity and SERPINA5 in the blood such that lower levels of this protective SERPIN in the blood were associated with increased disease severity (Overmyer et al., 2021). A second multi-omic study identified SERPINA5 as one of the most inversely-correlated proteins associated with high C-reactive protein (CRP) levels in COVID-19 patients (Sullivan et al., 2021). Taken together, these studies suggest that higher levels of SERPINA5 in the blood may help to mitigate COVID-19 disease and further support the findings from the present study.

Analysis of the effect of post-meditation plasma on infection with SARS-CoV-2 pseudovirus variants revealed significant protection for the Delta variant and D614G mutant (Fig. 4a, f). Interestingly, while only experienced post-meditation plasma was able to afford protection from Delta, only novice plasma was effective at lowering D614G infectivity. These data suggest that other factors in post-meditation plasma in addition to SERPINA5 may be contributing to the protective effects. It is noteworthy that post-meditation plasma from experienced meditators had a significant effect on lowering Delta variant infectivity (Fig. 4a). This variant was shown in previous work to be sixfold less sensitive to serum-neutralizing antibodies from recovered individuals and eightfold less sensitive to vaccine-generated antibodies as compared with the D614G variant, a mutant of the wild-type Wuhan-1 virus (Mlcochova et al., 2021). The present study indicates that Delta entry is inhibited by SERPINA5, likely by irreversible inhibition of TMPRSS2. Consistent with these observations, a recent study by Meng et al. has shown that deletion of TMPRSS2 had a major effect on Delta cleavage and entry (Meng et al., 2022). Taken together, these data suggest that while vaccination may be less effective for abrogating Delta infectivity, advanced meditation practice may help mitigate it via an increase in plasma SERPINA5. We conclude that SARS-CoV-2 vaccination in combination with meditation may be the best outcome with respect to SARS-CoV-2 infection and COVID-19 disease.

While this study presents important findings regarding meditation-induced factors that may regulate SARS-CoV-2 infection and COVID-19, several limitations must be noted. Firstly, while all study subjects were offered the same food for breakfast and lunch, we did not record any food diaries. Thus, while the assumption was made that all subjects ate a similar diet, it is possible that their diet varied within the choice of foods offered as well as total caloric intake. Secondly, for logistical reasons, pre- and post-retreat blood samples were collected after a short 30-min fast, not an overnight fast, potentially leading to some variability in blood samples. Thirdly, variables such as age, obesity, overall health, lifestyle, socioeconomic status, and pre-existing health conditions can influence the severity of COVID-19 disease. While meditation experience remained the primary focus of the analyses, it is possible that these other factors could play a role in one's response to meditation. Additionally, the data described in this research were collected after an intensive 7-day meditation experience. It is important to note that long-term benefits of meditation would undoubtedly require an ongoing meditation practice. Future studies will include longitudinal data collected from study subjects after the 7-day retreat to explore this point in more detail. Finally, the present data demonstrate that this specific guided meditation technique carried out in an immersive 7-day experience leads to a dramatic change in the expression of diverse plasma components with anti-viral properties, including SERPINA5. It remains unclear whether other mind-body practices would yield similar results. Future studies will assess the effect of other alternative practices such as yoga, breathwork, and other types of meditation including mindfulness meditation and mindfulness-based stress reduction techniques on the expression of plasma proteins that can enhance resiliency to SARS-CoV-2 infection and have a positive impact on COVID-19 disease.

4.1. Conclusions

Based on the current findings, overexpression of specific molecules may play a pivotal role in preventing or ameliorating viral infection and COVID-19 disease, suggesting that regular meditation practice has the potential to improve wellbeing and develop a healthy state through modulation of biological processes.

Author contributions

H.H.P, T.M.B., and J.D. conceived and designed the study. H.H.P. and J.P.Z.H. designed the experiments. T.M.B. was responsible for all clinical aspects of the study. J.H.Z.H., R. Chitteti, J.A.B., E.L.K., and G. B. provided technical support for cell-based assays. J.P.Z.H., R. Chitteti, R. Cuomo, and B.K.R. performed statistical analyses. S.S. performed molecular modeling studies. J.O., S.M., and D.J.G. carried out proteomics analysis. I.R.N. performed E.M. and S.E.M. analysis. A.M. prepared plasmids used in cell-based assays, J.M. carried out study subject recruitment. H.D.H. and C.S. designed the survey. R. Cuomo performed the analysis of survey data. J.H.Z.H., R. Chitteti, R. Cuomo, and S.S. created the figures. H.H.P, J.P.Z.H, M.A.P., R. Cuomo, and S.S. drafted the manuscript. H.H.P, J.P.Z.H, M.A.P., S.S., and J.D. critically reviewed the manuscript. H.H.P. and M.A.P. prepared the final version of the manuscript.

Declaration of competing interest

Dr. Joe Dispenza's company, Encephalon, runs the meditation retreats. All other authors have no conflicts of interest.

Data availability

Data will be made available on request.

Acknowledgments

We would like to thank Nathaniel Landau at NYU Langone for kindly providing the lambda variant plasmid as a gift. We thank Give to Give and InnerScience Research Fund for their generous support of this research. Dr. Patel was supported by a Research Career Scientist Award from the Veterans Administration (BX005229).

Appendix A. Supplementary data

Supplementary data to this article can be found online at https://doi.org/10.1016/j.bbih.2023.100675.

References

Azouz, N.P., et al., 2021. Alpha 1 antitrypsin is an inhibitor of the SARS-CoV-2-priming protease TMPRSS2. Pathog Immun 6, 55–74.
Bai, X., et al., 2021. Hypothesis: alpha-1-antitrypsin is a promising treatment option for COVID-19. Med. Hypotheses 146, 110394.
Berman, H.M., et al., 2000. The protein data bank. Nucleic Acids Res. 28, 235–242.
Bhasin, M.K., et al., 2013. Relaxation response induces temporal transcriptome changes in energy metabolism, insulin secretion and inflammatory pathways. PLoS One 8, e62817.
Bishara, D., Kalafatis, C., Taylor, D., 2020. Emerging and experimental treatments for COVID-19 and drug interactions with psychotropic agents. Ther Adv Psychopharmacol 10, 2045125320935306.
Black, D.S., Christodoulou, G., Cole, S., 2019. Mindfulness meditation and gene expression: a hypothesis-generating framework. Curr Opin Psychol 28, 302–306.
Bohlmeijer, E., Prenger, R., Taal, E., Cuijpers, P., 2010. The effects of mindfulness-based stress reduction therapy on mental health of adults with a chronic medical disease: a meta-analysis. J. Psychosom. Res. 68, 539–544.
Buonfrate, D., et al., 2022. High dose ivermectin for the early treatment of COVID-19 (COVER study): a randomised, double-blind, multicentre, phase II, dose-finding, proof of concept clinical trial. Int. J. Antimicrob. Agents, 106516. https://doi.org/10.1016/j.ijantimicag.2021.106516.
Buric, I., Farias, M., Jong, J., Mee, C., Brazil, I.A., 2017. What is the molecular signature of mind-body interventions? A systematic review of gene expression changes induced by meditation and related practices. Front. Immunol. 8, 670.
Bushell, W., et al., 2020. Meditation and yoga practices as potential adjunctive treatment of SARS-CoV-2 infection and COVID-19: a brief overview of key subjects. J. Alternative Compl. Med. 26, 547–556.
Chandran, V., et al., 2021. Large-scale genomic study reveals robust activation of the immune system following advanced Inner Engineering meditation retreat. Proc. Natl. Acad. Sci. U.S.A. 118.
Chang, B.H., Dusek, J.A., Benson, H., 2011. Psychobiological changes from relaxation response elicitation: long-term practitioners vs. novices. Psychosomatics 52, 550–559.
Comeau, S.R., Gatchell, D.W., Vajda, S., Camacho, C.J., 2004. ClusPro: a fully automated algorithm for protein-protein docking. Nucleic Acids Res. 32, W96–W99.
Elshikha, A.S., et al., 2016. Alpha 1 antitrypsin inhibits dendritic cell activation and attenuates nephritis in a mouse model of lupus. PLoS One 11, e0156583.
Elshikha, A.S., et al., 2018. Alpha 1 antitrypsin gene therapy extends the lifespan of lupus-prone mice. Mol Ther Methods Clin Dev 11, 131–142.
Epel, E.S., et al., 2016. Meditation and vacation effects have an impact on disease-associated molecular phenotypes. Transl. Psychiatry 6, e880.
Eyre, D.W., et al., 2022. Effect of covid-19 vaccination on transmission of alpha and Delta variants. N. Engl. J. Med. 386, 744–756.
Feng, H., Zhang, Y.B., Gui, J.F., Lemon, S.M., Yamane, D., 2021. Interferon regulatory factor 1 (IRF1) and anti-pathogen innate immune responses. PLoS Pathog. 17, e1009220.
Consortium, WHOST, Pan, H, Peto, R, et al., 2021. Repurposed Antiviral Drugs for Covid-19 - Interim WHO Solidarity Trial Results. N Engl J Med 384, 497–511.
G. 11.1.5, https:www.(geneious.com).
Glazik, R., et al., 2021. A snapshot of the practicality and barriers to COVID-19 interventions: public health and healthcare workers' perceptions in high and low- and middle-income countries. PLoS One 16, e0260041.
Gomutbutra, P., Yingchankul, N., Chattipakorn, N., Chattipakorn, S., Srisurapanont, M., 2020. The effect of mindfulness-based intervention on brain-derived neurotrophic factor (BDNF): a systematic review and meta-analysis of controlled trials. Front. Psychol. 11, 2209.
Jalkanen, P., et al., 2021. COVID-19 mRNA vaccine induced antibody responses against three SARS-CoV-2 variants. Nat. Commun. 12, 3991.
Kelly-Robinson, G.A., et al., 2021. The serpin superfamily and their role in the regulation and dysfunction of serine protease activity in COPD and other chronic lung diseases. Int. J. Mol. Sci. 22.
Li, Z., Jaroszewski, L., Iyer, M., Sedova, M., Godzik, A., 2020. Fatcat 2.0: towards a better understanding of the structural diversity of proteins. Nucleic Acids Res. 48, W60–W64.
Li, X.L., Wang, P., Xie, Y., 2021. Protease nexin-1 protects against Alzheimer's disease by regulating the sonic hedgehog signaling pathway. Int. J. Neurosci. 131, 1087–1096.
Lorincz, R., Curiel, D.T., 2020. Advances in alpha-1 antitrypsin gene therapy. Am. J. Respir. Cell Mol. Biol. 63, 560–570.
Lucas, A., Yaron, J.R., Zhang, L., Ambadapadi, S., 2018. Overview of serpins and their roles in biological systems. Methods Mol. Biol. 1826, 1–7.
Mashiach, E., Schneidman-Duhovny, D., Andrusier, N., Nussinov, R., Wolfson, H.J., 2008. FireDock: a web server for fast interaction refinement in molecular docking. Nucleic Acids Res. 36, W229–W232.
McKee, C.M., et al., 2012. Protease nexin 1 inhibits hedgehog signaling in prostate adenocarcinoma. J. Clin. Invest. 122, 4025–4036.
Meng, B., et al., 2022. Altered TMPRSS2 usage by SARS-CoV-2 Omicron impacts infectivity and fusogenicity. Nature 603, 706–714.
Mkaouar, H., et al., 2019. Serine protease inhibitors and human wellbeing interplay: new insights for old friends. PeerJ 7, e7224.
Mlcochova, P., et al., 2021. SARS-CoV-2 B.1.617.2 Delta variant replication and immune evasion. Nature 599, 114–119.
Omer, S.B., et al., 2021. Promoting COVID-19 vaccine acceptance: recommendations from the lancet commission on vaccine refusal, acceptance, and demand in the USA. Lancet 398, 2186–2192.
Ortigoza, M.B., et al., 2021. Efficacy and safety of COVID-19 convalescent plasma in hospitalized patients: a randomized clinical trial. JAMA Intern. Med. https://doi.org/10.1001/jamainternmed.2021.6850.
Ospina, M.B., et al., 2007. Meditation practices for health: state of the research. Evid. Rep. Technol. Assess. 1–263.
Overmyer, K.A., et al., 2021. Large-Scale multi-omic analysis of COVID-19 severity. Cell Syst 12, 23–40 e27.
Pawlowski, C., et al., 2021. FDA-authorized mRNA COVID-19 vaccines are effective per real-world evidence synthesized across a multi-state health system. Méd. 2, 979–992 e978.
Raman, R., Patel, K.J., Ranjan, K., 2021. COVID-19: unmasking emerging SARS-CoV-2 variants, vaccines and therapeutic strategies. Biomolecules 11.
Renckens, R., et al., 2007. Plasminogen activator inhibitor type 1 is protective during severe Gram-negative pneumonia. Blood 109, 1593–1601.
Sanrattana, W., Maas, C., de Maat, S., 2019. SERPINs-from trap to treatment. Front. Med. 6, 25.
Shapiro, S.L., 2009. The integration of mindfulness and psychology. J. Clin. Psychol. 65, 555–560.
Sullivan, K.D., et al., 2021. The COVIDome Explorer researcher portal. Cell Rep. 36, 109527.
J. H. University, Coronavirus Resource Center. (https://coronavirus.jhu.edu/map.html).
Wettstein, L., et al., 2021. Alpha-1 antitrypsin inhibits TMPRSS2 protease activity and SARS-CoV-2 infection. Nat. Commun. 12, 1726.
Wojta, J., 2020. Macrophages and thrombin-another link between inflammation and coagulation. Thromb. Haemostasis 120, 537.